

Mixed convection boundary layer flow about a solid sphere with Newtonian heating

M. Z. SALLEH¹⁾, R. NAZAR²⁾, I. POP³⁾

¹⁾ *Faculty of Industrial Science and Technology
Universiti Malaysia Pahang,
Lebuhraya Tun Abd Razak
26300 UMP Kuantan, Pahang, Malaysia*

²⁾ *School of Mathematical Sciences
Faculty of Science and Technology
Universiti Kebangsaan Malaysia
43600 UKM Bangi, Selangor, Malaysia
E-mail: rmn72my@yahoo.com*

³⁾ *Faculty of Mathematics
University of Cluj
R-3400 Cluj, CP 253, Romania*

IN THIS PAPER, the steady mixed convection boundary layer flow about a solid sphere, generated by Newtonian heating in which the heat transfer from the surface is proportional to the local surface temperature, is considered. The governing boundary layer equations are first transformed into a system of non-dimensional equations via the non-dimensional variables, and then into non-similar equations before they are solved numerically, using an implicit finite-difference scheme known as the Keller-box method. Numerical solutions are obtained for the skin friction coefficient and the wall temperature, as well as the velocity and temperature profiles with several parameters considered, namely the mixed convection parameter λ , the Prandtl number Pr and the conjugate parameter γ .

Copyright © 2010 by IPPT PAN

Notations

a radius of the sphere,
 h_s coefficient of proportionality for the surface heat flux,
 C_f skin friction coefficient,
 f dimensionless stream function,
 g acceleration due to gravity,
Gr Grashof number,
 k thermal conductivity,
Pr Prandtl number,
 q_w surface heat flux,
Re Reynolds number,

- T fluid temperature,
- T_w surface temperature,
- T_∞ ambient temperature,
- U_w velocity of the surface,
- U_∞ free stream velocity,
- u, v velocity components along the x and y directions, respectively,
- $u_e(x)$ velocity of the external flow,
- $u_w(x)$ velocity of the surface,
- x, y Cartesian coordinates along the surface and normal to it, respectively.

Greek letters

- α thermal diffusivity,
- β thermal expansion coefficient,
- γ conjugate parameter for Newtonian heating,
- θ dimensionless temperature,
- ν kinematic viscosity,
- λ mixed convection parameter,
- μ dynamic viscosity,
- ρ fluid density,
- ψ stream function.

1. Introduction

The analysis of heat transfer through a laminar boundary layer in the free, forced and mixed convection flow over a body of arbitrary shape and arbitrarily specified surface temperature or surface heat flux, constitutes a very important problem in the field of heat transfer and has received extensive attention. The prediction of heat transfer under such conditions encompasses a wide range of technological applications, such as the cooling problems in turbine blades or electronic systems, the calculation of heat transfer from bodies moving through the atmosphere, manufacturing processes, process industries, etc. (see YAHIO [1]). To the best of our knowledge, the only such studies which have been reported are the pioneering experimental work of YUGE [2] and the analytical work of HIEBER and GEBHART [3]. These studies, both experimental and analytical, were conducted under the action of very small Reynolds and Grashof numbers. CHEN and MUCOGLU [4, 5] have later studied mixed convection over a sphere with uniform surface temperature and uniform surface heat flux for very large Reynolds Re and Grashof numbers Gr , using the boundary layer approximations. The solution depends on the non-dimensional mixed convection parameter $\lambda = Gr/Re^2$. The Prandtl number considered is 0.7. Later, the mixed convection boundary layer flow about a solid sphere has been considered by many investigators in various ways. WONG *et al.* [6] solved the full Navier–Stokes and energy equation of an isothermal sphere in combined convection by a finite element method. MINKOWYCZ *et al.* [7] considered the mixed convection about a non-isothermal cylinder and sphere in a porous medium and

later, KUMARI and NATH [8] studied the unsteady mixed convection with double diffusion over a horizontal cylinder and sphere within a porous medium. In 2002, ANTAR and EL-SHAARAWI [9] studied the mixed convection around a liquid sphere in an air stream, in which they considered both aiding and opposing natural convection and the effect of the controlling parameters on engineering quantities such as the shear stress and the Nusselt number. NAZAR *et al.* [10, 11, 12] studied the mixed convection boundary layer flow about a solid sphere with constant surface temperature and constant heat flux in viscous and micropolar fluids, respectively. They carried out a very similar study as CHEN and MUCOGLU [4] for two values of the Prandtl number $Pr = 0.7$ and 7. Quite recently, YACOB and NAZAR [13] considered the mixed convection boundary layer on a solid sphere with constant surface heat flux, and followed by KOTOUČ *et al.* [14] who studied the loss of axisymmetry in the mixed convection (assisting flow) past a heated sphere. We mention also the relatively recent papers on this problem by JENNY and DUŠEK [15], JENNY *et al.* [16], MOGRABI and BAR-ZIV [17, 18] and MEBAREK *et al.* [19]. A detailed list of references on convective heat transfer problems can also be found in the recent book by POP and INGHAM [20].

In general, there are three common heating processes representing the constant wall temperature (CWT), constant heat flux (CHF), and conjugate conditions, where the heat transfer through a bounding surface of finite thickness and finite heat capacity is specified. The interface temperature is not known a priori but depends on the intrinsic properties of the system, namely, the thermal conductivities of the fluid and solid. In Newtonian heating (NH), the rate of heat transfer from the bounding surface with a finite heat capacity is proportional to the local surface temperature, and it is usually termed the conjugate convective flow. The Newtonian heating conditions have been used only recently by MERKIN [21], LESNIC *et al.* [22, 23, 24] and POP *et al.* [25], to study the free convection boundary layer over vertical and horizontal surfaces as well as over a small inclined flat plate from the horizontal surface embedded in a porous medium. The asymptotic solution near the leading edge and the full numerical solution along the whole plate domain have been obtained numerically, whilst the asymptotic solution far downstream along the plate has been obtained analytically. CHAUDHARY and JAIN [26, 27] studied the unsteady free convection boundary layer flow past an impulsively started, vertical infinite flat plate with Newtonian heating. Recently, SALLEH *et al.* [28, 29, 30] employed an implicit finite-difference scheme, namely the Keller-box method to obtain numerical solutions for the free convection boundary layer flow over a horizontal circular cylinder and sphere with Newtonian heating and the forced convection boundary layer flow at a forward stagnation point with Newtonian heating, respectively.

Therefore, the aim of the present paper is to study the mixed convection boundary layer flow about a solid sphere with Newtonian heating. The governing boundary layer equations are first transformed into a system of non-dimensional equations via the non-dimensional variables, and then into non-similar equations before they are solved numerically by the Keller-box method, as described in the books by NA [31] and CEBECI and BRADSHAW [32]. To the best of our knowledge, this problem has not been considered before for the case of Newtonian heating, so that the reported results are new.

2. Mathematical formulation

Here we consider the problem of steady mixed convection boundary layer flow about a solid sphere for the case of Newtonian heating, where the heat transfer rate from the bounding surface with a finite heat capacity is proportional to the local surface temperature and which is usually termed conjugate convective flow, as it was first proposed by MERKIN [21],

$$(2.1) \quad \left(\frac{\partial T}{\partial \bar{y}} \right)_{\bar{y}=0} = -h_s T_w,$$

where T_w is the unknown local surface temperature and h_s is a coefficient of proportionality for the surface heat flux. This configuration can arise in many important engineering devices which are termed conjugate flows, whereby heat is supplied to the convecting fluid through a bounding surface with a finite heat capacity, see [33, 34] for example. Alternatively, this set-up can model the heat transfer when there is a weak exothermic catalytic reaction taking place on the surface, generating heat at a rate proportional to the surface temperature. This is a reasonable assumption when the difference between the surface temperatures arising from the reaction and the ambient temperature are small, the situation envisaged in this paper. Other situations can occur in heat exchanger systems, where the conduction in solid tube wall is greatly influenced by the convection in the fluid flowing over it; in conjugate heat transfer around fins where the conduction within the fin and the convection in the fluid surrounding it, must be simultaneously analyzed in order to obtain vital design information; and in convective flows set-up when the bounding surfaces absorbs heat by solar radiation (LESNIC *et al.* [24]). The convective forced flow is assumed to be moving upwards, while the gravity vector g acts downwards in the opposite direction as shown in Figure 1, where the coordinates \bar{x} and \bar{y} are chosen such that \bar{x} measures the distance along the surface of the sphere from the lower stagnation point and \bar{y} measures the distance normal to the surface of the sphere. Under the Boussinesq and boundary layer approximations, the basic equations are

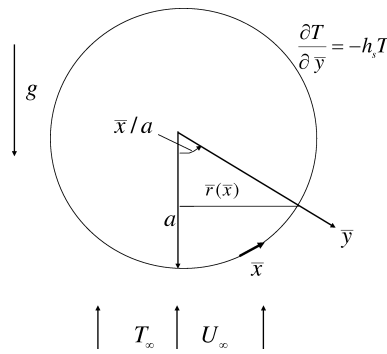


FIG. 1. Physical model and coordinate system.

$$(2.2) \quad \frac{\partial}{\partial \bar{x}}(\bar{r}\bar{u}) + \frac{\partial}{\partial \bar{y}}(\bar{r}\bar{v}) = 0,$$

$$(2.3) \quad \bar{u}\frac{\partial \bar{u}}{\partial \bar{x}} + \bar{v}\frac{\partial \bar{u}}{\partial \bar{y}} = \bar{u}_e\frac{d\bar{u}_e}{d\bar{x}} + \nu\frac{\partial^2 \bar{u}}{\partial \bar{y}^2} + g\beta(T - T_\infty)\sin\left(\frac{\bar{x}}{a}\right),$$

$$(2.4) \quad \bar{u}\frac{\partial T}{\partial \bar{x}} + \bar{v}\frac{\partial T}{\partial \bar{y}} = \alpha\frac{\partial^2 T}{\partial \bar{y}^2},$$

subject to the boundary conditions

$$(2.5) \quad \begin{aligned} \bar{u} = \bar{v} = 0, \quad \frac{\partial T}{\partial \bar{y}} = -h_s T \quad (\text{NH}) \quad \text{at } \bar{y} = 0, \\ \bar{u} \rightarrow 0, \quad T \rightarrow T_\infty \quad \text{as } \bar{y} \rightarrow \infty, \end{aligned}$$

where \bar{u} and \bar{v} are the velocity components along the \bar{x} and \bar{y} directions, respectively, T is the local temperature, T_∞ is the temperature of the ambient fluid, g is the gravity acceleration, $\alpha = \nu/\text{Pr}$ is the thermal diffusivity, β is the thermal expansion coefficient, $\nu = \mu/\rho$ is the kinematic viscosity, μ is the dynamic viscosity, ρ is the density and Pr is the Prandtl number. Let $\bar{r}(\bar{x})$ be the radial distance from the symmetrical axis to the surface of the sphere and $\bar{u}_e(\bar{x})$ be the local free stream velocity, which are given by

$$(2.6) \quad \bar{r}(\bar{x}) = a \sin\left(\frac{\bar{x}}{a}\right), \quad \bar{u}_e(\bar{x}) = \frac{3}{2}U_\infty \sin\left(\frac{\bar{x}}{a}\right).$$

However, for the sake of comparison, we shall also consider the classical cases of constant wall temperature (CWT), $T = T_w$ and constant surface heat flux (CHF), $\partial T/\partial y = -q_w/k$ at $y = 0$, where T_w is the constant wall temperature, q_w is the constant heat flux from the wall and k is the thermal conductivity.

We introduce now the following non-dimensional variables:

$$(2.7) \quad \begin{aligned} x &= \frac{\bar{x}}{a}, & y &= \text{Re}^{1/2} \left(\frac{\bar{y}}{a} \right), & r(x) &= \frac{\bar{r}(\bar{x})}{a}, & u &= \frac{\bar{u}}{U_\infty}, \\ u_e(x) &= \frac{\bar{u}_e(\bar{x})}{U_\infty}, & v &= \text{Re}^{1/2} \left(\frac{\bar{v}}{U_\infty} \right), & \theta &= \frac{T - T_\infty}{T_\infty} \quad (\text{NH}), \end{aligned}$$

where $\text{Re} = U_\infty a / \nu$ is the Reynolds number and we use $\theta = (T - T_\infty) / T_\infty$ (for CWT) and $\theta = (k / (aq_w)) \text{Re}^{1/2} (T - T_\infty)$ (for CHF). Substituting variables (2.7) into Eqs. (2.2)–(2.4), they become

$$(2.8) \quad \frac{\partial}{\partial x}(ru) + \frac{\partial}{\partial y}(rv) = 0,$$

$$(2.9) \quad u \frac{\partial u}{\partial x} + v \frac{\partial u}{\partial y} = u_e \frac{du_e}{dx} + \frac{\partial^2 u}{\partial y^2} + \lambda \theta \sin x,$$

$$(2.10) \quad u \frac{\partial \theta}{\partial x} + v \frac{\partial \theta}{\partial y} = \frac{1}{\text{Pr}} \frac{\partial^2 \theta}{\partial y^2},$$

and the boundary conditions (2.5) become (see [35]):

$$(2.11) \quad \begin{aligned} u = v = 0, & \quad \frac{\partial \theta}{\partial y} = -\gamma(1 + \theta) \quad (\text{NH}) \quad \text{at} \quad y = 0, \\ u_e(x) &\rightarrow \frac{3}{2} \sin x, \quad \theta \rightarrow 0 \quad \text{as} \quad y \rightarrow \infty, \end{aligned}$$

where $\gamma = ah_s \text{Re}^{-1/2}$ represents the conjugate parameter for Newtonian heating. We have noticed that (2.11) gives $\theta = 0$ when $\gamma = 0$, corresponding to having $h_s = 0$ and hence no heating from the sphere exists. On the other hand, λ is the mixed convection parameter which is given by

$$(2.12) \quad \lambda = \frac{\text{Gr}}{\text{Re}^2} (\text{NH, CWT}) \quad \text{or} \quad \lambda = \frac{\text{Gr}}{\text{Re}^{5/2}} (\text{CHF}),$$

and Gr is the Grashof number which is given by

$$(2.13) \quad \begin{aligned} \text{Gr} &= g\beta T_\infty \frac{a^3}{\nu^2} \quad (\text{NH}), & \text{or} & \quad \text{Gr} = g\beta(T_w - T_\infty) \frac{a^3}{\nu^2} \quad (\text{CWT}), & \text{or} \\ \text{Gr} &= g\beta \left(\frac{aq_w}{k} \right) \frac{a^3}{\nu^2} \quad (\text{CHF}). \end{aligned}$$

It is worth mentioning that in both cases of CWT and CHF, $\lambda > 0$ is for the aiding or assisting flow (heated sphere) and $\lambda < 0$ is for the opposing flow (cooled sphere), while for the present case of NH, the value of λ considered is only for $\lambda > 0$. For very small $|\lambda|$, forced convection effects dominate, while for large $|\lambda|$

it is the natural or free convection which is important. To solve Eqs. (2.8)–(2.10), subjected to the boundary conditions (2.11), we assume the following variables:

$$(2.14) \quad \psi = xr(x)f(x, y), \quad \theta = \theta(x, y),$$

where ψ is the stream function defined as

$$(2.15) \quad u = \frac{1}{r} \frac{\partial \psi}{\partial y} \quad \text{and} \quad v = -\frac{1}{r} \frac{\partial \psi}{\partial x},$$

so that Eqs. (2.9) and (2.10) then become

$$(2.16) \quad \frac{\partial^3 f}{\partial y^3} + \left(1 + \frac{x}{\sin x} \cos x\right) f \frac{\partial^2 f}{\partial y^2} - \left(\frac{\partial f}{\partial y}\right)^2 + \lambda \frac{\sin x}{x} \theta + \frac{9 \sin x \cos x}{4x} = x \left(\frac{\partial f}{\partial y} \frac{\partial^2 f}{\partial x \partial y} - \frac{\partial f}{\partial x} \frac{\partial^2 f}{\partial y^2} \right),$$

$$(2.17) \quad \frac{1}{\text{Pr}} \frac{\partial^2 \theta}{\partial y^2} + \left(1 + \frac{x}{\sin x} \cos x\right) f \frac{\partial \theta}{\partial y} = x \left(\frac{\partial f}{\partial y} \frac{\partial \theta}{\partial x} - \frac{\partial f}{\partial x} \frac{\partial \theta}{\partial y} \right),$$

subject to the boundary conditions

$$(2.18) \quad \begin{aligned} f = \frac{\partial f}{\partial y} = 0, \quad \frac{\partial \theta}{\partial y} = -\gamma(1 + \theta) \text{ (NH)} \quad \text{at } y = 0, \\ \frac{\partial f}{\partial y} \rightarrow \frac{3 \sin x}{2x}, \quad \theta \rightarrow 0 \quad \text{as } y \rightarrow \infty, \end{aligned}$$

along with $\theta(0) = 1$ (CWT) and $\theta'(0) = -1$ (CHF).

It can be seen that at the lower stagnation point of the sphere, $x \approx 0$, Eqs. (2.16) and (2.17) reduce to the following ordinary differential equations:

$$(2.19) \quad f''' + 2ff'' - f'^2 + \lambda\theta + \frac{9}{4} = 0,$$

$$(2.20) \quad \frac{1}{\text{Pr}} \theta'' + 2f\theta' = 0,$$

and the boundary conditions become

$$(2.21) \quad \begin{aligned} f(0) = f'(0) = 0, \quad \theta'(0) = -\gamma(1 + \theta(0)) \text{ (NH)}, \\ f' \rightarrow \frac{3}{2}, \quad \theta \rightarrow 0 \quad \text{as } y \rightarrow \infty, \end{aligned}$$

where primes denote differentiation with respect to y .

The quantities of physical interest in this problem are the skin friction coefficient, C_f and the wall temperature, $\theta_w(x)$, which are given by

$$(2.22) \quad \text{Re}^{1/2} C_f = x \frac{\partial^2 f}{\partial y^2}(x, 0), \quad \theta_w(x) = -1 - \frac{\partial \theta}{\partial y}(x, 0).$$

where $C_f = \tau_w / (\rho U_\infty^2)$ and $\tau_w = \mu(\partial \bar{u} / \partial \bar{y})_{\bar{y}=0}$ is the wall shear stress.

3. Solution procedure

Equations (2.16) and (2.17) subject to boundary conditions (2.18) are solved numerically using the Keller-box method as described in the books by NA [31] and CEBECI and BRADSHAW [32]. The solution is obtained in the following four steps:

- reduce Eqs. (2.16) and (2.17) to a first-order system,
- write the difference equations using central differences,
- linearize the resulting algebraic equations by Newton's method, and write them in the matrix-vector form,
- solve the linear system by the block triadiagonal elimination technique (see SALLEH *et al.* [36] and ISHAK *et al.* [37] for the details of this method).

4. Results and discussion

Equations (2.16) and (2.17) subject to the boundary conditions (2.18) were solved numerically using an efficient, implicit finite-difference method known as the Keller-box scheme for the cases of CWT, CHF and NH with several parameters considered, namely, the mixed convection parameter λ , the Prandtl number Pr , the conjugate parameter γ and the coordinate running along the surface of the sphere, x . The numerical solutions start at the lower stagnation point of the sphere, $x \approx 0$, with initial profiles as given by Eqs. (2.19) and (2.20) and proceed round the sphere up to 120° (see NAZAR *et al.* [10, 11]). Values of Pr considered are $Pr = 0.7, 1$ and 7 . It is worth mentioning that small values of Pr ($\ll 1$) physically correspond to liquid metals, which have high thermal conductivity but low viscosity, while large values of Pr ($\gg 1$) correspond to high-viscosity oils. It is also worth to be pointed out that specifically, the Prandtl number considered in this study, namely $Pr = 0.7, 1.0$ and 7.0 , correspond to air, electrolyte solution and water, respectively.

At the lower stagnation point of the sphere, $x \approx 0$, due to the decoupled boundary layer equations (2.19) and (2.20) when the mixed convection parameter $\lambda = 0$ (forced convection), there is a unique value of the reduced skin friction coefficient, $f''(0) = 2.4104$ for all Prandtl numbers Pr , which is in good agreement with the value $f''(0) = 2.4151$ found by NAZAR *et al.* [10, 11] by using the Keller-box method as well as the series solutions.

The values of $f''(0)$, $-\theta'(0)$ and $\theta(0)$ for the cases of CWT and CHF, are shown in Tables 1 and 2, respectively. Some numerical results obtained by an implicit finite-difference scheme as reported by NAZAR *et al.* [10, 11] for the cases of CWT and CHF, are also included in these tables for comparison purposes. It is found that the agreement between the previously published results with the present ones is very good. We can conclude that this numerical method works

Table 1. Values of $f''(0)$ and $-\theta'(0)$ for various values of λ when $Pr = 0.7$ (CWT).

λ	$f''(0)$		$-\theta'(0)$	
	NAZAR <i>et al.</i> [10]	Present	NAZAR <i>et al.</i> [10]	Present
-4.6	0.0770	0.0699	0.6011	0.5990
-4.5	0.1566	0.1544	0.6117	0.6115
-4.0	0.5028	0.4996	0.6534	0.6528
-3.0	1.0700	1.0664	0.7108	0.7099
-2.0	1.5581	1.5542	0.7529	0.7519
-1.0	2.0016	1.9973	0.7870	0.7860
-0.5	2.2115	2.2070	0.8021	0.8010
0.0	2.4151	2.4104	0.8162	0.8150
1.0	2.8064	2.8012	0.8463	0.8406
2.0	3.1804	3.1745	0.8648	0.8636
3.0	3.5401	3.5336	0.8857	0.8845
4.0	3.8880	3.8807	0.9050	0.9038
5.0	4.2257	4.2177	0.9230	0.9217
6.0	4.5546	4.5457	0.9397	0.9385
7.0	4.8756	4.8659	0.9555	0.9542
8.0	5.1896	5.1791	0.9704	0.9691
9.0	5.4974	5.4859	0.9846	0.9833
10.0	5.7995	5.7870	0.9981	0.9967
20.0	8.5876	8.5647	1.1077	1.1061

Table 2. Values of $f''(0)$ and $\theta(0)$ for various values of λ when $Pr = 0.7$ (CHF).

λ	$f''(0)$		$\theta(0)$	
	NAZAR <i>et al.</i> [11]	Present	NAZAR <i>et al.</i> [11]	Present
-2.8	0.0791	0.0669	1.6504	1.6567
-1.5	1.5620	1.5560	1.3277	1.3302
-1.0	1.8785	1.8731	1.2856	1.2878
-0.5	2.1592	2.1541	1.2525	1.2545
0.0	2.4151	2.4104	1.2252	1.2270
0.5	2.6526	2.6478	1.2020	1.2038
1.0	2.8756	2.8707	1.1818	1.1834
2.0	3.2881	3.2830	1.1479	1.1494
3.0	-	3.6613	-	1.1214
4.0	-	4.0136	-	1.0977
5.0	4.3515	4.3451	1.0759	1.0773
6.0	-	4.6602	-	1.0591
7.0	-	4.9606	-	1.0430
8.0	-	5.249	-	1.0284
9.0	-	5.5272	-	1.0151
10.0	5.8046	5.7954	1.0017	1.0029
20.0	8.1431	8.1273	0.9160	0.9171

efficiently for the present problem and we are also confident that the results presented here are accurate.

For the case of NH, the values of $f''(0)$ and $\theta(0)$ obtained numerically by solving Eqs. (2.19) and (2.20) subject to boundary conditions (2.21) for various values of λ when $\gamma = 1$ and $\text{Pr} = 0.7, 1$ and 7 , are presented in Tables 3 and 4, respectively. It can be seen from these tables that the values of $f''(0)$ and $\theta(0)$ are higher for $\text{Pr} = 0.7$ than those for $\text{Pr} = 1$ and 7 .

Further, Tables 5 to 10 show the numerical values of C_f and $\theta_w(x)$ at the different positions of x for different values of λ when $\gamma = 1$ and $\text{Pr} = 0.7, 1$ and 7 , respectively. It can be seen from these tables that the values of C_f and $\theta_w(x)$ are higher for $\text{Pr} = 0.7$ than for $\text{Pr} = 7$, when the parameter x and λ are fixed. It is also seen from these tables that $\theta_w(x)$ decreases as the mixed convection parameter, λ , increases. Also, for a given value of λ , the skin friction coefficient C_f and the wall temperature $\theta_w(x)$ are seen to increase with increasing the distance x from the stagnation point. Further, we can see from these tables that, increasing of λ delays the separation and that separation can be completely suppressed in the range $0 \leq x \leq 120^\circ$ for sufficiently large values of λ (> 0). The actual value of

Table 3. Values of $f''(0)$ and $\theta(0)$ for various values of λ when $\text{Pr} = 0.7$ and 1 , and $\gamma = 1$ (NH).

λ	$\text{Pr} = 0.7$		$\text{Pr} = 1$	
	$f''(0)$	$\theta(0)$	$f''(0)$	$\theta(0)$
0.01	5.8834	1032.4011	3.3748	274.6189
0.02	5.9061	520.1127	3.4225	144.4513
0.03	5.9269	349.0227	3.4683	100.9444
0.04	5.9491	263.6847	3.5101	78.7904
0.05	5.9694	212.2873	3.5485	65.4268
0.1	6.0716	109.6156	3.7186	37.9501
0.5	6.7525	26.6476	4.3491	28.9103
1.0	7.4152	15.7022	5.2161	8.7364
2.0	8.4538	9.7883	6.1773	6.0929
3.0	9.2945	7.6114	6.9258	5.0014
4.0	10.0216	6.4336	7.5625	4.3714
5.0	10.6723	5.6782	8.1273	3.9495
6.0	11.2669	5.1456	8.6407	3.6419
7.0	11.8173	4.7431	9.1151	3.4047
8.0	12.3355	4.4287	9.5584	3.2147
9.0	12.8236	4.1733	9.9763	3.0580
10.0	13.2876	3.9609	10.3730	2.9258
20.0	17.0966	2.8658	13.6177	2.2136

Table 4. Values of $f''(0)$ and $\theta(0)$ for various values of λ when $Pr = 7$ and $\gamma = 1$ (NH).

λ	Pr = 7	
	$f''(0)$	$\theta(0)$
0.05	2.4235	1.1174
0.1	2.4365	1.1141
0.5	2.5378	1.0933
1.0	2.6579	1.0709
2.0	2.8808	1.0326
3.0	3.0854	1.0009
4.0	3.2760	0.9739
5.0	3.4552	0.9503
6.0	3.6249	0.9296
7.0	3.7867	0.9110
8.0	3.9415	0.8943
9.0	4.0904	0.8790
10.0	4.2340	0.8651
20.0	5.4682	0.7679

Table 5. Values of C_f at the different positions x for various values of λ when $Pr = 0.7$ and $\gamma = 1$.

λ x_s	C_f				
	0.01	0.02	0.04	1	7
0°	0.0000	0.0000	0.0000	0.0000	0.0000
10°	2.4247	2.4143	2.4192	2.5549	3.0281
20°	5.1300	5.1086	5.1168	5.3448	6.2020
30°	7.7607	7.7283	7.7395	8.0487	9.2646
40°	10.4076	10.3645	10.3784	10.7600	12.3109
50°	12.8475	12.7946	12.8110	13.2593	15.1916
60°	15.2483	15.0594	15.0779	15.5847	18.0592
70°	17.3454	17.2749	17.2954	17.8562	20.8610
80°	19.2011	19.1229	19.1451	19.7677	23.1955
90°		20.8530	20.8766	21.5858	25.2947
100°		22.0944	22.1192	22.9133	26.7892
110°			23.1678	24.0142	27.9605
120°			23.5698	24.4255	28.3528

Table 6. Values of $\theta_w(x)$ at the different positions x for various values of λ when $Pr = 0.7$ and $\gamma = 1$.

λ x_s	$\theta_w(x)$				
	0.01	0.02	0.04	1	7
0°	1032.4011	520.1127	263.6847	15.7022	4.7431
10°	4593.8650	2279.8779	1143.2143	49.4303	9.1384
20°	4932.8780	2448.5298	1227.1952	52.3580	9.4377
30°	5135.8530	2549.5688	1277.5526	54.1713	9.6484
40°	5309.2326	2635.8811	1320.6215	55.7855	9.8618
50°	5484.3107	2723.0335	1364.5369	57.4712	10.0882
60°	5675.1214	2815.1750	1410.2106	59.2949	10.2630
70°	5885.0581	2922.5078	1463.8869	61.4519	10.4711
80°	6134.9920	3046.9182	1526.1240	63.9607	10.7660
90°		3193.0798	1599.2579	66.8564	11.1646
100°		3367.0696	1686.3283	70.2466	11.6790
110°			1791.3590	74.3284	12.3286
120°			1920.3443	79.3798	13.1477

Table 7. Values of C_f at the different positions x for various values of λ when $Pr = 1$ and $\gamma = 1$.

λ x_s	C_f				
	0.01	0.03	0.06	0.1	2
0°	0.0000	0.0000	0.0000	0.0000	0.0000
10°	1.4834	1.4934	1.5062	1.5214	1.7821
20°	3.2056	3.2216	3.2422	3.2667	3.7124
30°	4.8554	4.8765	4.9038	4.9363	5.5491
40°	6.5608	6.5861	6.6190	6.6584	7.4212
50°	8.0932	8.1223	8.1603	8.2059	9.1097
60°	9.5454	9.5777	9.6200	9.6709	10.7082
70°	10.9992	11.0342	11.0803	11.1359	12.3647
80°		12.1980	12.3642	12.3070	13.7480
90°		13.3567	13.4085	13.4714	15.0774
100°			14.1970	14.2624	15.9685
110°			14.9453	15.0122	16.7488
120°				15.2655	16.9774

Table 8. Values of $\theta_w(x)$ at the different positions x for various values of λ when $Pr = 1$ and $\gamma = 1$.

λ x_s	$\theta_w(x)$				
	0.01	0.03	0.06	0.1	2
0°	2742.3120	100.8235	56.4181	37.9501	6.0929
10°	2556.4810	859.8126	434.8734	264.4599	16.6862
20°	2793.4136	937.5609	472.9940	286.8403	17.4648
30°	2931.8003	983.1001	495.4030	300.0423	17.9706
40°	3045.9184	1020.7964	514.0432	311.0866	18.4440
50°	3158.1121	1057.9828	532.5109	322.0844	18.9597
60°	3274.3028	1096.5915	551.7461	333.5819	19.5281
70°	3407.9159	1141.0687	573.9547	346.8912	20.1585
80°		1192.2899	600.3492	362.2686	20.8382
90°		1252.1177	629.5182	380.2685	21.6373
100°			664.9468	401.5768	22.6267
110°			707.3675	427.1015	23.8709
120°				458.3454	25.4522

Table 9. Values of C_f at the different positions x for various values of λ when $Pr = 7$ and $\gamma = 1$.

λ x_s	C_f				
	0.01	0.02	0.03	0.1	3
0°	0.0000	0.0000	0.0000	0.0000	0.0000
10°		0.1119	0.1139	0.1352	0.4705
20°		0.3326	0.3361	0.3614	1.0377
30°		0.3945	0.3992	0.4319	1.4934
40°		0.6322	0.6337	0.6718	2.0614
50°		0.6543	0.6572	0.7091	2.4761
60°		0.8914	0.7710	0.8397	2.9584
70°		1.0050	1.0096	1.0922	3.5252
80°			0.9784	1.0762	3.9618
90°			1.2065	1.3108	4.3058
100°			1.1202	1.2352	4.4679
110°			1.3184	1.4360	4.7778
120°			1.1603	1.2842	4.7417

Table 10. Values of $\theta_w(x)$ at the different positions x for various values of λ when $Pr = 7$ and $\gamma = 1$.

λ x_s	$\theta_w(x)$				
	0.01	0.02	0.03	0.1	3
0°	1.1118	1.1219	1.1193	1.1139	2.1872
10°		43.1846	30.1700	10.5022	8.8129
20°		46.2051	32.2326	10.2346	9.2373
30°		48.8039	33.7935	10.1297	9.5529
40°		50.2278	34.3635	10.1304	9.7932
50°		51.6119	35.2579	10.2852	10.0785
60°		53.1400	36.3028	10.4855	10.3337
70°		55.0546	37.5999	10.7531	10.6022
80°			39.2765	11.1334	10.9429
90°			41.2613	11.6064	11.3547
100°			43.8152	12.2376	11.8991
110°			46.9797	13.0352	12.5949
120°			51.1374	14.0961	13.4929

$\lambda = \lambda_k$, which first gives no separation, is difficult to determine exactly as it has to be found by successive integrations of the equations. However, the numerical solutions indicate that the value of λ which first gives no separation, lies between 0.02 and 0.04 for $Pr = 0.7$, lies between 0.06 and 0.1 for $Pr = 1$, while for $Pr = 7$ the value of λ lies between 0.02 and 0.03.

Figure 2 illustrates the variation of the wall temperature $\theta_w(x)$ with Prandtl number Pr when $\lambda = 1$ and $\gamma = 1$. To get a physically acceptable solution, Pr must be greater than the critical value, say $Pr_c = Pr_c(\gamma)$, i.e. $Pr > Pr_c(\gamma)$. It can be seen from this figure that $\theta_w(x)$ becomes large (unbounded) as Pr approaches the critical value $Pr_c \cong 0.0169$ when $\lambda = 1$ and $\gamma = 1$.

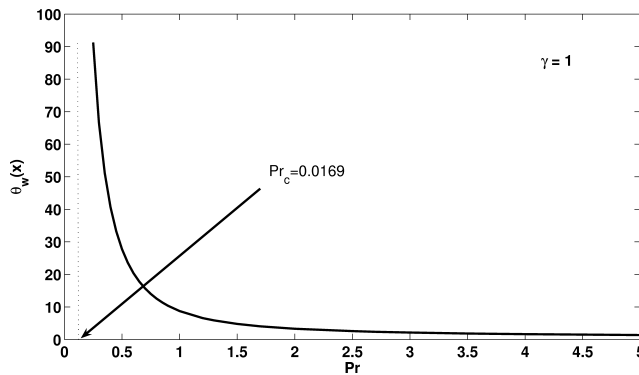


FIG. 2. Variation of the wall temperature with Prandtl number Pr when $\lambda = 1$ and $\gamma = 1$.

Figure 3 shows the variation of the wall temperature $\theta_w(x)$ with the conjugate parameter γ when $\text{Pr} = 1$ and $\lambda = 1$. Also, to get a physically acceptable solution, γ must be less than a certain critical value, say $\gamma_c = \gamma_c(\text{Pr})$, i.e. $\gamma < \gamma_c(\text{Pr})$. It can be seen from this figure that $\theta_w(x)$ becomes large (unbounded) as γ approaches the critical value $\gamma_c \cong 3.522$ when $\text{Pr} = 1$ and $\lambda = 1$.

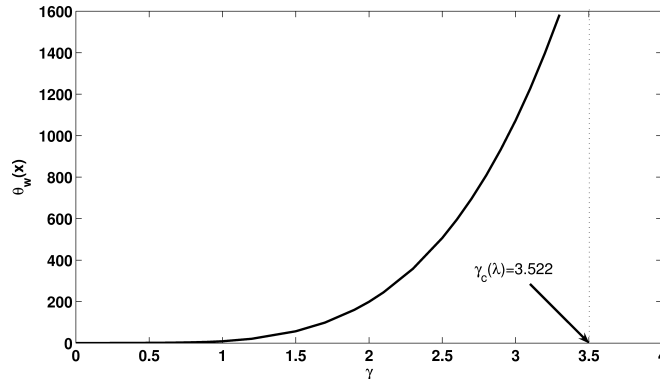


FIG. 3. Variation of the wall temperature with conjugate parameter γ when $\lambda = 1$ and $\text{Pr} = 1$.

It should be pointed out that from the boundary conditions (2.5), we must have $(\partial T / \partial \bar{y})_{\bar{y}=0} < 0$, as the applied heating condition is given in terms of the physical fluid temperature T , not of a temperature difference. Therefore, we can only have physically acceptable solutions of the Eqs. (2.16) and (2.17) subject to the boundary conditions (2.18), which have $(\partial \theta / \partial y)_{y=0} < 0$. But we will further refer to Eqs. (2.19) and (2.20) with the boundary conditions (2.21). From these equations, in order to have $\theta'(0) < 0$ it means that we can have solutions only when $\gamma < \gamma_c$ (γ_c is the critical value of γ), where the solutions become unbounded, for the existence of mixed convection solution with the Newtonian heating given by (2.11) or (2.21). This is shown in Figs. 2 and 3.

The velocity and temperature profiles near the lower stagnation point, $x \approx 0$, are given in Figs. 4 to 6 for some values of λ when $\text{Pr} = 0.7$ and $\gamma = 1$. We found that for fixed values of Pr and γ , the velocity profiles increase, while the temperature profiles decrease when the mixed convection parameter λ increases. From Fig. 4 it is noticed that there are overshoots of the velocity profiles when $\lambda \geq 1$ where these overshoots take place higher for $\lambda = 10$ than for $\lambda = 1$.

The velocity and temperature profiles near the lower stagnation point of the sphere, $x \approx 0$, for some values of Pr when $\lambda = 1.0$ and $\gamma = 1$, are plotted in Figs. 7 and 8. It can be seen from these figures that, as Pr increases, both the velocity and temperature profiles decrease. At large Pr , the thermal boundary layer is thinner than at a smaller Pr . This is because for small values of Pr ($\ll 1$),

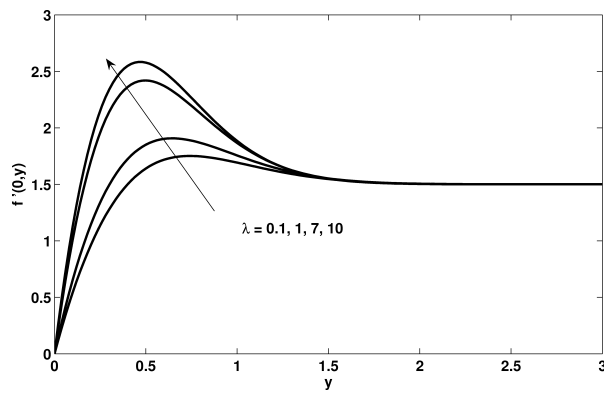


FIG. 4. Velocity profiles near the lower stagnation point of the sphere, $x \approx 0$, for various values of λ when $Pr = 0.7$ and $\gamma = 1$.

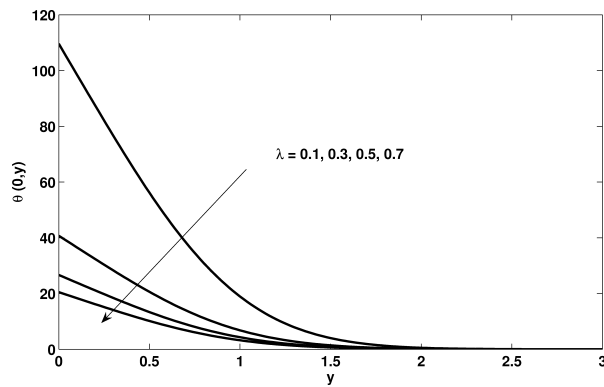


FIG. 5. Temperature profiles near the lower stagnation point of the sphere, $x \approx 0$, for various values of $\lambda (\ll 1)$ when $Pr = 0.7$ and $\gamma = 1$.

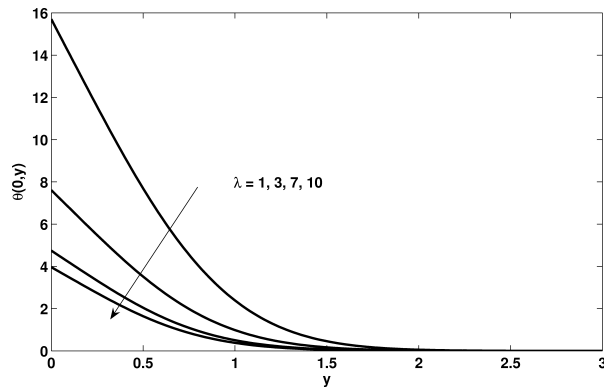


FIG. 6. Temperature profiles near the lower stagnation point of the sphere, $x \approx 0$, for various values of $\lambda (\gg 1)$ when $Pr = 0.7$ and $\gamma = 1$.

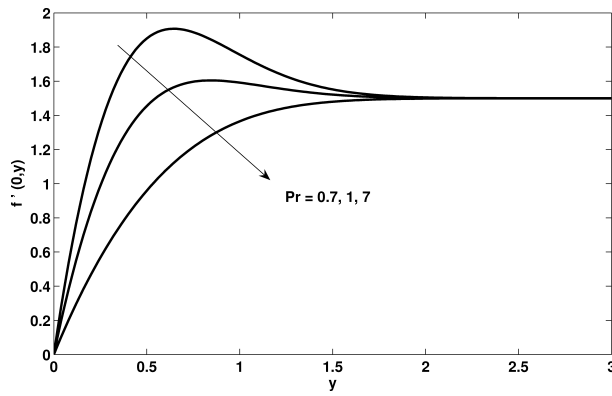


FIG. 7. Velocity profiles near the lower stagnation point of the sphere, $x \approx 0$, for various values of Pr when $\lambda = 1.0$ and $\gamma = 1$.

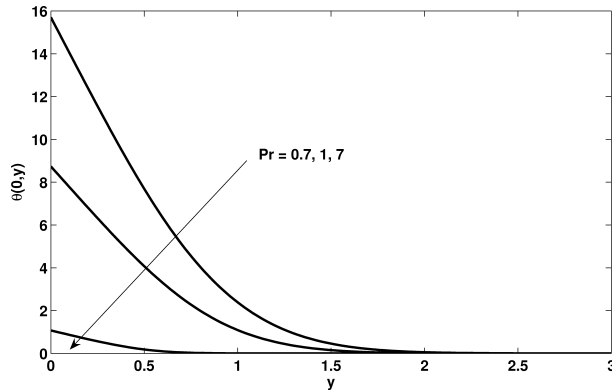


FIG. 8. Temperature profiles near the lower stagnation point of the sphere, $x \approx 0$, for various values of Pr when $\lambda = 1.0$ and $\gamma = 1$

the fluid is highly conductive. Physically, if Pr increases, the thermal diffusivity decreases and these phenomena lead to decreasing of the energy ability that reduces the thermal boundary layer. From Fig. 7 it is also noticed that there are overshoots of the velocity profiles when $Pr \leq 1$ where these overshoots take place higher for $Pr = 0.7$ than for $Pr = 1$.

Further, Figs. 9 and 10 illustrate the variation of $\theta_w(x)$ at different positions x for different values of λ , when $\gamma = 1$ and $Pr = 0.7$ and 1, respectively. It can be seen from these figures that the values of $\theta_w(x)$ are higher for $Pr = 0.7$ than $Pr = 1$, when the parameters x and λ are fixed. It is also found that $\theta_w(x)$ decreases as the mixed convection parameter increases and $\theta_w(x)$ is seen to increase with increasing of the distance x from the stagnation point of the sphere, $x \approx 0$.

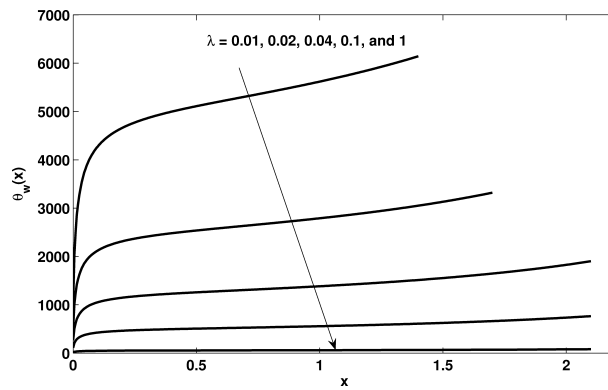


FIG. 9. Variation of the wall temperature $\theta_w(x)$ with x for various values of λ when $Pr = 0.7$ and $\gamma = 1$.

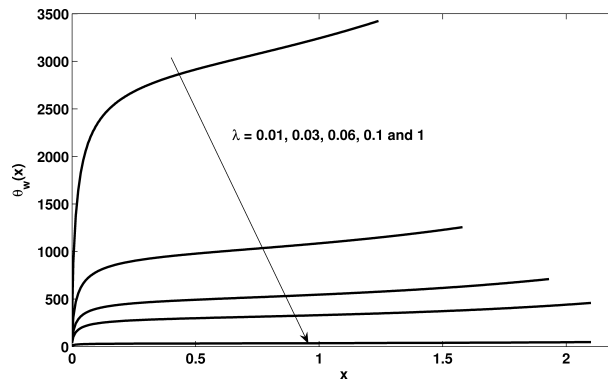


FIG. 10. Variation of the wall temperature $\theta_w(x)$ with x for various values of λ when $Pr = 1$ and $\gamma = 1$.

5. Conclusions

In this paper, we have numerically studied the problem of mixed convection boundary layer flow of a solid sphere with Newtonian heating (NH). It is shown how the mixed convection parameter λ , the Prandtl number Pr and the conjugate parameter γ , affect the skin friction coefficient, the wall temperature and the velocity and temperature profiles. We can conclude that (for the case of NH):

- an increase of the value of Pr leads to a decrease of both the velocity and temperature profiles;
- near the lower stagnation point of the sphere, when λ increases, the velocity profiles increase but the temperature profiles decrease;

- there are overshoots of the velocity profiles near the lower stagnation point of the sphere from the free stream velocity;
- an increase of the value of Pr and λ leads to a decrease of the wall temperature, $\theta_w(x)$;
- to get a physically acceptable solution, Pr must be greater than Pr_c (critical value of Pr) depending on γ , and also γ must be less than γ_c (critical value of γ) depending on Pr .

Acknowledgements

The authors gratefully acknowledge the financial supports received from the Ministry of Higher Education, Malaysia (UKM-ST-07-FRGSS0036-2009) and research grant (RDU090308) from the Universiti Malaysia Pahang. The authors would also like to thank the reviewers for the valuable comments and suggestions.

References

1. L.S. YAO, *Buoyancy Effects on a Boundary Layer along an Infinite Vertical Cylinder with a Step Change of Surface Temperature*, In: *Winter Annual Meeting of ASME* November 16–18, Chicago, Illinois. Paper 80– WA/HT **25**, 1981.
2. T. YUGE, *Experiments on Heat Transfer from Sphere Including Combined Natural and Forced Convection*, *J. Heat Transfer*, **82**, 214–220, 1960.
3. C.A. HIEBER, B. GEBHART, *Mixed Convection from a Sphere at Small Reynolds and Grashof Numbers*, *J. Fluid Mech.*, **38**, 137–159, 1969.
4. T.S. CHEN, A. MUCOGLU, *Analysis of Mixed Forced and Free Convection about a Sphere*, *Int. J. Heat Mass Transfer*, **20**, 867–875, 1977.
5. T.S. CHEN, A. MUCOGLU, *Mixed Convection about a Sphere with Uniform Surface Heat Flux*, *J. Heat Transfer*, **100**, 542–544, 1978.
6. K.L. WONG, S.C. LEE, C.K. CHEN, *Finite Element Solution of Laminar Combined Convection from a Sphere*, *J. Heat Transfer*, **108**, 860–865, 1986.
7. W.J. MINKOWYCZ, P. CHENG, C.H. CHANG, *Mixed Convection about a Nonisothermal Cylinder and Sphere in a Porous Medium*, *Numerical Heat Transfer*, **8**, 349–359, 1985.
8. M. KUMARI, G. NATH, *Unsteady Mixed Convection with Double Diffusion over a Horizontal Cylinder and a Sphere within a Porous Medium*, *Wärme- und Stoffübertragung*, **24**, 103–109, 1989.
9. M.A. ANTAR, M.A.I. EL-SHAARAWI, *Mixed Convection around a Liquid Sphere in an Air Stream*, *Heat and Mass Transfer*, **38**, 419–424, 2002.
10. R. NAZAR, N. AMIN, I. POP, *On the Mixed Convection Boundary Layer Flow about a Solid Sphere with Constant Surface Temperature*, *The Arabian Journal for Science and Engineering*, **27**, 117–135, 2002.

11. R. NAZAR, N. AMIN, I. POP, *Mixed Convection Boundary Layer Flow from a Sphere with Constant Surface Heat Flux in a Micropolar Fluid*, Journal of Energy, Heat and Mass Transfer, **29**, 1129–1138, 2002.
12. R. NAZAR, N. AMIN, I. POP, *Mixed Convection Boundary Layer Flow about an Isothermal Sphere in a Micropolar Fluid*, Int. J. Thermal Sciences, **42**, 283–293, 2003.
13. N.A.M. YACOB, R.M. NAZAR, *Mixed Convection Boundary Layer on a Solid Sphere with Constant Surface Heat Flux*, Journal of Quality Measurement and Analysis, **2**, 63–74, 2006.
14. M. KOTOUČ, G. BOUCHET, J. DUŠEK, *Loss of Axisymmetry in the Mixed Convection, Assisting Flow Past a Heated Sphere*, Int. J. Heat and Mass Transfer, **51**, 2686–2700, 2008.
15. M. JENNY, J. DUŠEK, *Efficient Numerical Method for the Direct Numerical Simulation of the Flow past a Single Light Moving Spherical Body in Transitional Regimes*, J. Comput. Phys., **194**, 215–232, 2004.
16. M. JENNY, J. DUŠEK, G. BOUCHET, *Instabilities and Transition of a Sphere Falling or Ascending Freely in a Newtonian Fluid*, J. Fluid Mech., **508**, 201–239, 2004.
17. E. MOGRABI, BAR-ZIV, *Dynamics of a Spherical Particle in Mixed Convection Flow Field*, J. Aerosol Sci., **36**, 387–409, 2005.
18. E. MOGRABI, BAR-ZIV, *On the Mixed Convection Hydrodynamic Force on a Sphere*, J. Aerosol Sci., **36**, 1177–1181, 2005.
19. M. MEBAREK, G. BOUCHET, J. DUŠEK, *Hydrodynamic Forces Acting on a Rigid Fixed Sphere in Early Transitional Regimes*, Eur. J. Mech. B/Fluids, **25**, 321–336, 2006.
20. I. POP, D.B. INGHAM, *Convective Heat Transfer: Mathematical and Computational Modelling of Viscous Fluids and Porous Media*, Oxford, Pergamon, 2001.
21. J.H. MERKIN, *Natural Convection Boundary-layer Flow on a Vertical Surface with Newtonian Heating*, Int. J. Heat Fluid Flow, **15**, 392–398, 1992.
22. D. LESNIC, D.B. INGHAM, I. POP, *Free Convection Boundary Layer Flow along a Vertical Surface in a Porous Medium with Newtonian Heating*, Int. J. Heat Mass Transfer, **42**, 2621–2627, 1999.
23. D. LESNIC, D.B. INGHAM, I. POP, *Free Convection from a Horizontal Surface in a Porous Medium with Newtonian Heating*, J. Porous Media, **3**, 227–235, 2000.
24. D. LESNIC, D.B. INGHAM, I. POP, C. STORR, *Free Convection Boundary-layer Flow above a Nearly Horizontal Surface in a Porous Medium with Newtonian Heating*, Heat and Mass Transfer, **40**, 665–672, 2004.
25. I. POP, D. LESNIC, D.B. INGHAM, *Asymptotic Solutions for the Free Convection Boundary-layer Flow along a Vertical Surface in a Porous Medium with Newtonian Heating*, Hybrid Methods Engng., **2**, 31–40, 2000.
26. R.C. CHAUDHARY, PREETI JAIN, *Unsteady Free Convection Boundary-layer Flow Past an Impulsively Started Vertical Surface with Newtonian Heating*, Romanian J. Phys., **9**, 911–925, 2006.
27. R.C. CHAUDHARY, PREETI JAIN, *An Exact Solution to the Unsteady Free Convection Boundary-layer Flow Past an Impulsively Started Vertical Surface with Newtonian Heating*, Journal of Engineering Physics and Thermophysics, **80**, 954–960, 2007.

28. M.Z. SALLEH, R. NAZAR, *Free convection boundary layer flow over a horizontal circular cylinder with Newtonian heating*, Sains Malaysiana, **39**, 671–676, 2010.
29. M.Z. SALLEH, R. NAZAR, I. POP, *Forced Convection Boundary Layer Flow at a Forward Stagnation Point with Newtonian Heating*, Chemical Engineering Communications, **196**, 987–996, 2009.
30. M.Z. SALLEH, R. NAZAR, I. POP, *Modeling of Free Convection Boundary Layer Flow on a Sphere with Newtonian Heating*, Acta Applicandae Mathematicae, doi:10.1007/s10440-010-9567-5, 2010.
31. T.Y. NA, *Computational Methods in Engineering Boundary Value Problem*, New York: Academic Press, 1979.
32. T. CEBECI, P. BRADSHAW, *Physical and Computational Aspects of Convective Heat Transfer*, New York, Springer, 1984.
33. I. POP, J.K. SUNADA, P. CHENG, W.J. MINKOWYCZ, *Conjugate Free Convection from Long Vertical Plate Fins Embedded in a Porous Medium*, Int. J. Heat Mass Transfer, **28**, 1629–1636, 1985.
34. A. POZZI, M. LUPO, *The Coupling of Conduction with Laminar Natural Convection along a Flat Plate*, Int. J. Heat Mass Transfer, **31**, 1807–1814, 1988.
35. M.Z. SALLEH, R. NAZAR, N.M. ARIFIN, I. POP, J.H. MERKIN, *Forced Convection Heat Transfer over a Horizontal Circular Cylinder with Newtonian Heating*, J. Engineering Mathematics, 2009 (submitted).
36. M.Z. SALLEH, S. AHMAD, R. NAZAR, *Numerical Solution of the Forced Convection Boundary Layer Flow at a Forward Stagnation Point*, European J. Scientific Research, **19**, 644–653, 2008.
37. A. ISHAK, R. NAZAR, I. POP, *Post Stagnation-point Boundary Layer Flow and Mixed Convection Heat Transfer over a Vertical, Linearly Stretching Sheet*, Archives of Mechanics, **60**, 303–322, 2008.

Received September 23, 2009; revised version May 28, 2010.
